Nuclear Instruments and Methods in Physics Research A 378 (1996) 35–39

NUCLEAR INSTRUMENTS & METHODS IN PHYSICS RESEARCH Section A

ELSEVIER

Three-dimensional ion beam-profile monitor for storage rings

T. Quinteros[a,*], D.R. DeWitt[a], A. Paál[b], R. Schuch[a]

[a] *Atomic Physics Department, University of Stockholm, Frescativägen 24, S-104 05 Stockholm, Sweden*
[b] *Manne Siegbahn Laboratory, University of Stockholm, Frescativägen 24, S-104 05 Stockholm, Sweden*

Received 7 March 1996

Abstract

We have developed a non-destructive three-dimensional beam-profile monitor for storage rings. It allows the measurement of the complete profile of stored ion beams by simultaneously detecting electrons and ions created through ionisation of the residual gas. The horizontal coordinate of each point in the profile is determined by detecting the ionised electrons, guided in a strong magnetic field, on a two-dimensional position sensitive detector. The magnetic field assures precision in the determination of the absolute horizontal position of the ion beam and prevents the detection of background electrons originating outside the monitor's active volume. Simultaneously, the vertical coordinate of the beam distribution is obtained by measuring the time difference between the detection of the electrons and the recoil ions in coincidence. The time of flight spectrum shows the different components of the residual gas and allows an intrinsic calibration of the physical parameters. We present results of a test performed with an 8 MeV/u D^+ beam at the storage ring CRYRING in Stockholm.

1. Introduction

Non-destructive methods for monitoring circulating ion beams in storage rings are of importance for both beam adjustments and experiments. Commonly used devices are electrostatic pick-ups, to give information about the mean position of the beam, current transformers, to obtain the beam intensity, and Schottky noise detectors to monitor the beam revolution frequency, i.e. the beam energy, and the energy spread. Ring experiments using merged beams or ion-laser interactions require detailed information about the intensity distribution within the beam envelope. Beam-profile monitors are already in operation for this purpose. The monitor at LEAR [1] detects electrons produced in the ionisation of atoms from a gas jet crossing the beam. Other monitors use the products of residual gas ionisation to obtain a cross section of the stored beam. The detectors at TSR in Germany [2] and at KEK-PS, in Tokyo [3] detect recoil ions using a two-dimensional position sensitive detector. The previous model of the monitor at CRYRING [4], detected the ionised electrons with a two-dimensional anode and used the magnetic field of a bending magnet to lower the background and increase position resolution. Each of these devices can monitor one transversal direction of the ion-beam.

In this work, we report on the development of a monitor (BPM) for the beam-profile in three dimensions of a beam stored in a storage ring. The new device measures the complete beam profile by detecting, at the same time, the horizontal and vertical positions and density distribution of the ion-beam, along a 40 mm long path of the beam. This is done non-destructively, by detecting the horizontal coordinate of the beam intensity distribution from the electrons and the vertical coordinate from the time of flight of the recoil ion from the ionisation of residual gas atoms and molecules by the stored ions. The device has been tested with an 8 MeV/u D^+ ion beam at the storage ring CRYRING.

2. Experimental technique

The monitor, schematised in Fig. 1, consists of two opposing detectors, located above and below the circulating beam. Each of them is a multichannel plate chevron assembly (MCP) of 40 mm diameter active area. One detector is equipped with a two-dimensional resistive anode and the other with a conductive anode. The horizontal and vertical profiles of the stored ion beam are measured simultaneously by detecting the products of ionisation of residual gas molecules by the stored particles. The position sensitive detector is used to detect the ionised electrons and the other for the recoil ions. The extraction voltages are applied to 90% transmission grids located 3 mm in front of each detector. During the test, the grid of the electron detector was grounded while the grid at the ion detector was set at voltages ranging between −34 V

* Corresponding author. Tel.: +46 8 859511, fax: +46 8 158674, e-mail: quinteros@msi.se.

PII S0168-9002(96)00278-1

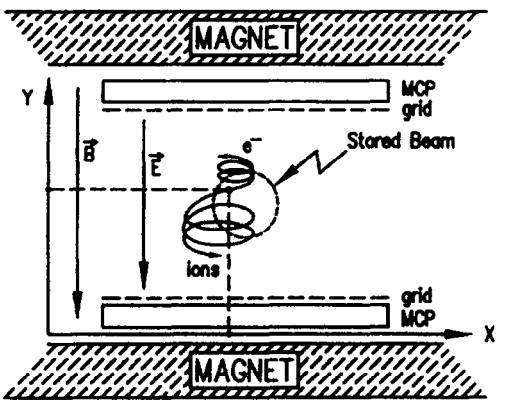

Fig. 1. Schematic of the beam-profile monitor. The stored beam ionises the residual gas atoms. The products of the ionisation are driven electrostatically towards the multichannel plate detectors following helicoidal trajectories around the magnetic field lines.

and +150 V to analyse variations in the time-of-flight. The front of the electron detector was set to +1 kV and the front of the ion detector to −2.2 kV. With these acceleration potentials, the detection efficiency was about 80% for electrons and at least 50% for ions.

The location of the ionised electron when it impacts the position sensitive detector gives the horizontal coordinate of the ionisation event [4]. The vertical coordinate is obtained by measuring the time difference between the detection of the ionised electron and recoiling ion in coincidence. Fig. 2 shows, schematically, the location of the beam-profile monitor installed at CRYRING [5]. The device is installed in the gap of the dipole magnet located just after the electron cooler and was operated at magnetic fields of 0.6–0.7 T. The monitor can be set up in the homogeneous magnetic field of any dedicated magnet. The figure also shows the location of another multichannel plate detector mounted in the straight line after the electron cooler. This device, which detects neutrals produced by recombination with electrons in the cooler, was used to compare the ion beam profiles with those obtained with the beam-profile monitor.

Positioning the BPM assembly in a strong homogeneous magnetic field ensures an accurate determination of the absolute horizontal position of the ionisation event and avoids the detection of background electrons originating outside the active volume of the detector, electrons which would otherwise flood the detector. The trajectories of the ionisation products are helixes around the magnetic field lines. The mean electron energy expected for electrons ionised by an 8 MeV/u D^+ ion beam is 100 eV [6], which gives an average electron cyclotron radius of 50 μm in the 0.7 T magnetic field required to store the beam at this energy. With a nominal position resolution of the multichannel plate chevron detectors of ~100 μm, the estimated horizontal position resolution is ~112 μm.

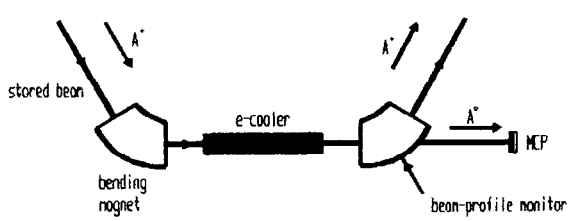

Fig. 2. Schematic of the section of CRYRING showing the electron cooler, the positions of the beam-profile monitor and the position sensitive detector (MCP) used to detect neutral atoms A^0 produced by recombination of stored ions A^+ in the electron cooler.

Since the gaps of the dipole magnets are the smallest vertical apertures of the storage ring (54 mm at CRYRING), the gap between the detectors, when placed in one of the dipoles, limits the vertical angular acceptance of the ring. Thus, each detector unit must be as thin as possible. For that reason, the housing of each detector, including the front grid, is designed with a total thickness of 12 mm. The thickness of the aluminium oxide pieces used as isolators had to be 0.8 mm/kV or larger to avoid discharges through tracking along their surface. This has been a limiting factor in the compact design of the detectors housing . The gap between the detectors is 24.5 mm, similar to the size of the ion beam at injection. Therefore, the device must be retracted during injection and acceleration and reinserted when the beam is cooled. The reduction in the minimal aperture of the ring can, in some cases, lead to a shortening of the ion-beam's lifetime. This is the case for light ion beams, for which the lifetime can be determined by single large angle scattering of the stored ions by residual gas atoms. In the case of heavy ions, losses in the beam intensity are mainly due to electron loss, recombination or capture, and do not depend on the ring's apertures. A more detailed discussion of the effects of a reduced aperture on the beam lifetime has been presented in Ref. [4].

Since the applied extraction field is constant, the time difference between the detection of electrons and ions is given by

$$T = \sqrt{\frac{2MDx}{q\,\Delta V}} - \sqrt{\frac{2mD(D-x)}{e\,\Delta V}}\,. \qquad (1)$$

The first term accounts for the time of flight (TOF) of the recoil ion from the position of the ionisation event (x) to the lower detector, and the second term is the TOF of the ionised electron to the upper multichannel plate. In Eq. (1), D represents the distance between the detectors in the active volume of the device, ΔV the effective extraction voltage and M and m the masses of the ionisation products. Thus, the vertical position of the ionisation events can be obtained from the measured time by inverting Eq. (1). The time of flight is determined by the mass of the recoil ion. Peaks for different gas components – of different masses M – show the actual composition of the residual gas in the region where the beam is stored. These peaks, properly identified, are used for on-line calibration.

During the test, the position and time–amplitude conversion (TAC) signals were recorded in list-mode to analyse and check the consistency of the data off-line. The recording of a list-mode event is triggered by a TAC valid conversion signal. For each event the four resistive anode amplitudes and TAC analog signal are recorded following analog to digital conversion. For routine measurements, the software for the inversion of Eq. (1) to obtain the vertical position can be implemented to give an on-line three-dimensional view of the beam.

The construction of a BPM which can be inserted in the gap of the dipole magnet under ultra high vacuum (UHV) conditions requires the detectors to be mounted on a long manipulator. In the present design of the setup the pre-amplifiers are positioned close to the detectors and connected to the detectors with unscreened non-impedance matched wires just 50 mm long. In this way we obtained a noise level low enough to allow the use of pulses from the back of the channel plates, with 20 ns rise time, as timing signal. The time resolution obtained, as discussed below, was ~40 ns. Placement of the pre-amplifiers so close to the detectors locate them inside the strong magnetic field which, however, did not affect their functioning in any noticeable way.

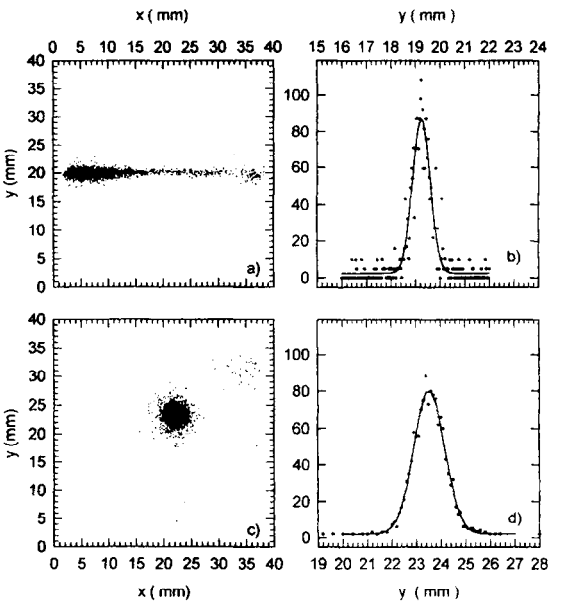

Fig. 3. (a) Horizontal beam profile of a 8 MeV/uD$^+$ ion beam. (b) A transversal projection of the counts in (a) from which a beam width of 0.8 mm (FWHM) was obtained. (c) Transversal section of the beam measured by a multichannel plate detector intercepting the neutrals after recombination in the electron cooler. (d) A transversal projection of (c) in the horizontal plane.

3. Results and discussion

The BPM has been tested with 8 MeV/u D^+ ions stored with an intensity of about 10 μA. At a pressure of 2×10^{-11} mbar in the region in which the detector was placed, the coincidence rate during the measurement was 250 Hz, in good agreement with the estimated 300 Hz at this pressure. The singles electron rate was about 1 kHz, larger than the coincidence rate due to dark counting and the detection of secondary electrons emitted from the detector housing. Fig. 3a shows the two-dimensional image of the ionised electrons on the position sensitive anode, representing the horizontal profile of the stored ion-beam, measured in coincidence with the ionised atoms. Fig. 3b, is a transversal projection of the counts in Fig. 3a. The beam width and the horizontal position, obtained as the FWHM and the mean value of a Gaussian curve fit to the data, were 0.80±0.15 and 19.2±0.1 mm respectively. The beam enters the active volume of the monitor from the left of the figure. The intensity of the counts on this side is higher and decreases along the beam path (z-axis). The time of flight analysis of the data has shown that, in the first 4.5 mm along this direction, the fraction of particles detected with $M/q = 2$ to the total rate is ten times larger than in the rest of the active area of the detector, and remains constant at other positions along the active area of the detector. This is probably caused by particles in the halo of the ion beam colliding with the detector housing. Fig. 3c is the transversal section of the beam detected by a neutrals detector located in the straight line after the electron cooler (MCP in Fig. 2). Fig. 3d shows a projection of the counts in Fig. 3c in the horizontal plane, indicating a beam diameter of 1.5±0.1 mm. The ion beam image observed by this detector, which is located approximately 4 m from the cooler, is expected to be somewhat larger than the actual beam due to the finite divergence of the beam.

Fig. 4 shows one time of flight (TOF) spectrum. This data was taken from the region $z > 5$ mm to insure

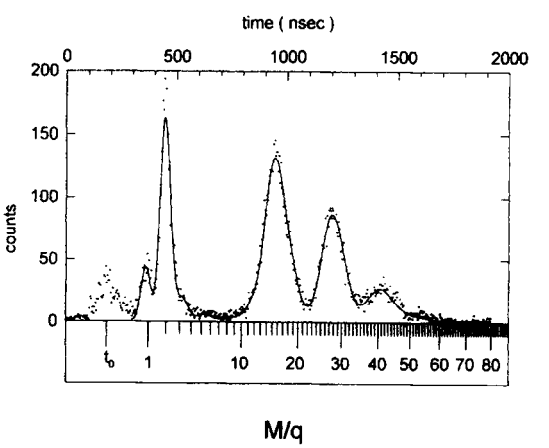

Fig. 4. Time of flight spectrum. The solid line is the result of a fit to obtain the contribution to the counts of each species of different M/q ratio (see text). The extraction voltage applied was −34 V. The lower axis shows the location of each M/q and the time offset t_0.

constant ratios of the various peaks. To further check the consistency of this data, separate TOF spectra were generated for each 5 mm interval between 5 and 40 mm. Although the statistics of each of these individual spectra is relatively low, these spectra will reveal any systematic effect which varies with z. The most important parameter in this regard is the slope of the beam as it passes through the detector. As shown by Eq. (1), the positions of the peaks will vary if the beam passes through the detector with a non-zero vertical angle. No such peak shift was observed, therefore the integrated spectra for $z > 5$ mm was used for the remaining analysis. The spectrum in Fig. 4 was obtained with an applied extraction voltage of −34 V. For further analysis several sets of data similar to that shown in Fig. 4 were taken with applied extraction voltages ranging from −34 V to 150 V.

The different peaks in Fig. 4 originate from the ionisation of different atoms and molecules according to their mass to charge ratios M/q. Identification of these peaks was made with the aid of a measurement of the background gas composition by a quadrupole mass spectrometer. The partial pressures thus obtained are listed in Table 1. The table also includes an estimate of the expected ion production ratios obtained using the respective ionisation cross sections calculated following Ref. [7]. Evaluation of the ion beam profile using the data of Fig. 4 proceeds in two steps: First, peak functions are fitted to the data to obtain the positions, intensities, and widths of the various M/q components. Second, a fit of Eq. (1) to the centroids of the M/q peaks is made to determine the parameters x and ΔV. We treat ΔV as a fit parameter because it has been found empirically that its value is not strictly equal to the voltage difference applied to the grids; we discuss this further below.

Inspection of the TOF peaks indicates that they are approximately Gaussians. The widths of the observed peaks are determined by three factors: (i) the width of the ion beam, transformed as in Eq. (1), (ii) the number of different atoms and molecules contained within them, and (iii) instrumental and electronic noise. Based on the apparent shapes of the peaks, we fit Gaussians to the spectrum. The Gaussians were related by the condition

$$\sigma(t) = \sqrt{\sigma_{M,q}^2 + \sigma_N^2}\,, \tag{2}$$

Table 1
Main components of the residual gas at CRYRING and the estimated contribution of each species to the ionisation rate

Gas	Mass	P (mbar)	% ionisation
H_2	2	9.9×10^{-12}	100
He	4	2.1×10^{-14}	0.2
CH_4	16	2.0×10^{-13}	10
H_2O	18	2.5×10^{-13}	9
CO	28	1.4×10^{-13}	5
Ar	40	8.3×10^{-14}	3
CO_2	44	3.2×10^{-14}	2

which was imposed on the standard deviations. Here $\sigma(t)$ is the standard deviation at t, σ_N describes the noise contribution to the width, which is assumed to be Gaussian, and

$$\sigma_{M,q} = \left.\frac{\partial T}{\partial x}\right|_{M,q} \sigma_x\,, \tag{3}$$

where σ_x is the standard deviation of the ion beam and $\sigma_{M,q}$ is the corresponding TOF peak width for an ion of mass to charge ratio M/q. Eq. (3) shows that the TOF peak increases with M/q, but the width increase is not as rapid as the increase of T due to the noise component. Note that $\sigma_{M,q}$ also varies with the extraction voltage and σ_x and σ_N remain constant.

The fit to the TOF spectrum includes σ_x and σ_N as variable parameters, along with a time offset to account for any fixed electronic delay unrelated to the TOF spectrum. We found that the observed spectrum could be described by 11 Gaussians. The fit is shown in Fig. 4. Although the fit is generally good, the results indicate that the noise contribution is larger than the beam-width contribution to the observed peaks, i.e. the Gaussians have widths which do not increase significantly with increasing M/q and decreasing ΔV. This precludes a precise determination of σ_x from the present data. For example, if we assume that $\sigma_x \approx \sigma_y$ we find from Eqs. (1) to (3) a value of 20 ns for σ_N, which contributes with 47 ns to the FWHM of the observed peaks which had a total width of 52 ns. The occurrence of this high noise level is attributed to the relatively weak timing signal produced by the position sensitive detector. This detector, which uses a resistive anode to map the position of an arriving electron, produces four slow linear signals to convey the position information.

Precise timing information cannot be obtained from these signals. Instead, the electron's time of arrival is obtained from the electrode which applies bias voltage to the face of the channel plate opposite the resistive anode; the time signal is generated by the pulse of electrons which are emitted by the channel plate. This pulse is fast but weak, and rides on a noise background of relatively significant amplitude.

The results of the second step of the analysis of the data in fig. 4 are shown in Fig. 5. The figure shows the result of a fit of Eq. (1) to the peak centroids obtained from the TOF spectrum. In order to fit to the centroids, an initial set of M/q ratios based on the data of Table 1 was selected. Fits to the initial set showed that some points deviated from the curve. The same points were found to consistently deviate from the fit curve regardless of the applied extraction voltage, indicating that their M/q ratios were incorrect. The figure shows the data points plotted and fit with M/q ratios which fall on the fit curve. The data points represent the molecules H^+, H_2^+, $^3He^+$, CH_4^+ and O^+, H_2O^+, CO^+, Ar^+, C^{2+}, O^{2+}, C^+, and a small contributor to the spectrum with $M/q = 52$, not clearly identified. The peak amplitudes observed in the spectrum seem to follow

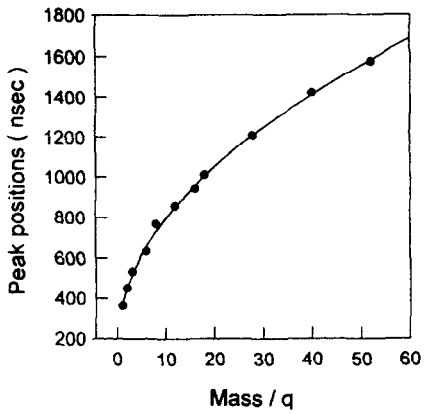

Fig. 5. Position of the time peaks identified as contributing to the time of flight spectrum in Fig. 4. The solid line is the expected dependence of the time of flight on the mass over charge ratio, as a result of the fit.

the characteristic distribution given by fractions of hydrocarbon chains, and may result from a local concentration of alcohols released from the BPM itself [8].

In attempting to fit Eq. (1) to the M/q data we found that the effective extraction voltage ΔV was significantly higher than the applied voltage. Regardless of the applied voltage the effective voltage was found to be in the 160 V range. This value of ΔV reduces the precision in the determination of the position (x), since the two parameters are tightly coupled in Eq. (1), and ΔV has a large uncertainty. The origin of this large effective extraction voltage is not clear. We speculate that the high voltage biases applied to the opposing channel plate assemblies may introduce offset voltages through unintended ground loops, shifting the voltages applied to the grids.

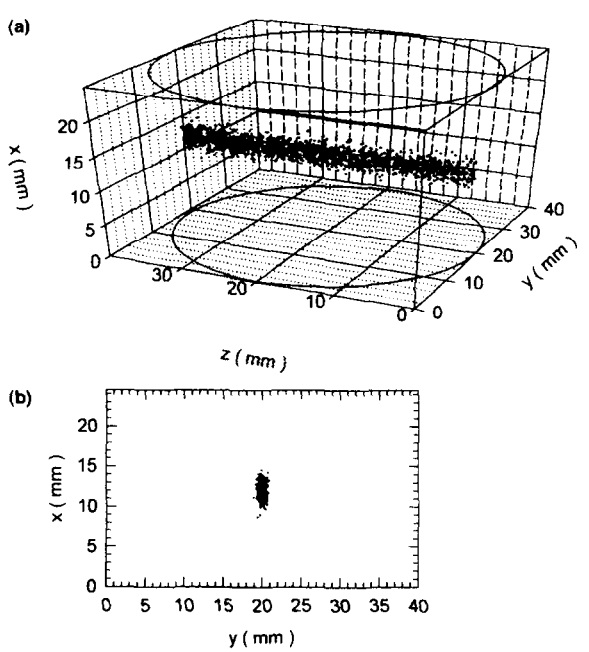

Fig. 6. (a) Three-dimensional image of an 8 MeV/u D^+ beam reconstructed as two Gaussian distributions in the horizontal and vertical planes, with mean values and widths obtained from the analysis of the data. (b) Transversal section of the image in (a).

The vertical profile can be obtained from the time spectrum by inverting Eq. (1) for one of the ionised species, with the effective voltage obtained from the fit described previously. Fig. 6 shows a three-dimensional image of the stored beam reconstructed as a Gaussian distribution with the mean values and the widths obtained from the analysis of the data. We estimate that the resolution required for complete separation of the H_2 peak can be achieved if the extraction voltage is reduced to 40 V or less. This should allow the construction of an on-line three-dimensional image of the stored ion beam in future experiments.

4. Conclusions

We have tested a non-destructive three-dimensional beam-profile monitor for ion storage rings. The horizontal and vertical positions and intensity distributions of a stored ion-beam were measured simultaneously by detecting the products of ionisation of the residual gas in a strong magnetic field. We have achieved an accuracy in the determination of the beam position of ~110 μm in the horizontal plane. The measured horizontal beam width (FWHM) was 0.80±0.15 mm. The time of flight analysis is consistent with the residual gas components, mainly H_2, CH_4, O_2 and H_2O, as measured with a quadrupole analyser. The time resolution achieved, ~40 ns, is expected to resolve a beam width of ~1 mm, with an extraction voltage of 40 V or less. This low effective extraction voltage could not be reached in the present setup.

References

[1] B. Vosicki and K. Zankel, IEEE 91 Part. Accel. Conf., eds. L. Lizama and J. Chew, vol. 5 (IEEE, New York, 1991) p. 2814.
[2] B. Hochadel, F. Halbrecht, M. Grieser, D. Habs, D. Schwalm, E. Szmola and A. Wolf, Nucl. Instr. and Meth. A 343 (1994) 401.
[3] T. Kawakubo, T. Ishida, E. Kadokura, Y. Ajima and T. Adachi, Nucl. Instr. and Meth. A 302 (1991) 397.
[4] T. Quinteros, R. Schuch, M. Pajek, P. Sigray, H. Cederquist, H. Danared, L. Bagge, A. Filevich, J. Jeansson, A. Källberg and A. Paál, Nucl. Instr. and Meth. A 333 (1993) 288.
[5] K. Abrahamsson et al., Nucl. Instr. and Meth. B 79 (1993) 269.
[6] R. Schuch, H. Schöne, P.D. Miller, H.F. Krause, P.F. Dittner, S. Datz and R.E. Olson, Phys. Rev. Lett. 60 (1988) 925.
[7] F.F. Rieke and W. Prepejchal, Phys. Rev. A 6 (1972) 1507.
[8] Balzers, Partial pressure measurement in vacuum technology, BG 800 169PE(8907).